International Journal of Chemical, Materials and Biomolecular Sciences
ISSN: 2415-6620
Vol:4, No:2, 2010

Microbial Leaching Process to Recover Valuable Metals from Spent Petroleum Catalyst Using Iron Oxidizing Bacteria

Debabrata Pradhan, Dong J. Kim, Jong G. Ahn, and Seoung W. Lee

***Abstract*—**Spent petroleum catalyst from Korean petrochemical industry contains trace amount of metals such as Ni, V and Mo. Therefore an attempt was made to recover those trace metal using bioleaching process. Different leaching parameters such as Fe(II) concentration, pulp density, pH, temperature and particle size of spent catalyst particle were studied to evaluate their effects on the leaching efficiency. All the three metal ions like Ni, V and Mo followed dual kinetics, i.e., initial faster followed by slower rate. The percentage of leaching efficiency of Ni and V were higher than Mo. The leaching process followed a diffusion controlled model and the product layer was observed to be impervious due to formation of ammonium jarosite $(NH_4)Fe_3(SO_4)_2(OH)_6$. In addition, the lower leaching efficiency of Mo was observed due to a hydrophobic coating of elemental sulfur over Mo matrix in the spent catalyst.

***Keywords*—**Bioleaching, diffusion control, shrinking core, spent petroleum catalyst.

I. Introduction

THE annual production of spent petroleum catalyst containing different metals is estimated to be 150,000-170,000 tons/year [1]. It is regarded as hazardous due to significant amounts of various heavy metal ions [2]. Several processes have been developed to recover metal values from waste petroleum catalyst [3-9]. The metal values can either be recovered through pyro or hydrometallurgical routes. In the pyrometallurgical route, various techniques are followed such as direct smelting, calcination and smelting, chlorination and salt roasting [3-5]. In the hydrometallurgical route, initially the waste material is roasted followed by either acid or alkali leaching [6-8]. Direct leaching of spent catalyst is also carried out at elevated pressure [9].

Debabrata Pradhan is with Korea Institute of Geoscience and Mineral Resources (KIGAM), Daejeon 305-350, South Korea (corresponding author's phone: +82-42-868-3592; fax: +82-42-868-3415; e-mail: dpradhan05@gmail.com).

Dong J. Kim and Jong G. Ahn are with Korea Institute of Geoscience and Mineral Resources (KIGAM), Daejeon 305-350, South Korea.

Seoung W. Lee is with Chungnam National University, Daejeon 305-764, South Korea.

Due to the several drawbacks of the conventional techniques described above, biotechnological leaching processes have been developed as potential alternative methods. The main advantage in the bio-hydro technique is the ease of operation as well as limited use of process control, thus making the operation more users friendly. Bioleaching studies of spent catalyst have been reported using different types of bacteria, both heterotrophic as well as autotrophic [10-13]. There are several factors which affect bioleaching kinetics such as pH, nutrient concentration, pulp density, reaction time, metal toxicity, temperature etc. The present communication describes the effect of various leaching parameters vis-à-vis leaching efficiency using a mixed iron oxidizing bacteria culture.

II. Materials and Methods

A. Preparation of Solid Sample Prior to Leaching

The collected spent petroleum catalyst was covered with oil which was removed by washing in acetone using a soxhlet extractor. The de-oiled mass was dried, ground and sieved to the required size fraction. The metal content in the waste was analyzed by ICP-AES (Jobin-Yvon JY 38). The typical chemical composition of the spent catalyst was as follows (wt%): Al, 19.5; S, 11.5; Ni, 2.0; V, 9.0; Mo, 1.4; Fe, 0.3.

B. Microorganisms

The water sample collected from an effluent pond at the Dalsung mine in south Korea was cultured in 9K media at pH of 1.8 [14]. The growth pattern of bacteria was observed by analyzing residual ferrous concentration in the growth media. The concentrations of ferrous in the medium was analyzed by a titration method using 0.1N potassium dichromate as titrant and barium diphenylamine-4-sulfonate (BDAS) as a redox indicator. All leaching studies were conducted using the active bacterial culture.

C. Bioleaching

All leaching experiments were conducted in 250 mL Erlenmeyer flasks containing 90 mL media and 10 mL inoculum in each. A centrifugal shaker-cum-incubator was

used with the speed fixed at 180 rpm. Periodically, samples were collected to determine the pH, Eh and metal ion concentrations. The metal content in leach liquor was analyzed by ICP-AES. The following leaching conditions were maintained unless otherwise specified: Fe(II),10 g/L; pulp density, 10%; pH, 2.0; temperature, 35 ^{o}C; particle size, 106 μm. All experiments were carried out in triplicate and the standard deviations of the results were found to be ± 5%.

III. Results and Discussion

A. Effect of Contact Time

Bioleaching studies were carried out for 15 days in order to optimize the leaching time. The results are shown in Fig. 1. The leaching kinetics for all the elements followed dual kinetics, i.e., initial faster rate followed by a slower rate. The initial faster kinetics accounted for around 60% and lasted around 4 days. The slower kinetics then continued upto 10 days and beyond that the leaching was negligible. Therefore, in all cases, the leaching studies were limited to 10 days. The dual rate of leaching may be due to either depletion of easily available reacting species or formation of product layer or diffusion limited like surface and intra-particle or combination of all. It was further observed that the leaching rate varied widely amongst the constituents as Ni and V showed similar leaching rates whereas Mo leached much slower. The slower Mo leaching rate may be due to various factors such as crystal structure and presence of a diffusion layer. Pradhan et al. [10] reported that Mo and Ni were present as sulfides (using XRD) and all other species (Al, V and Fe) were in their respective oxide form. The basic difference between sulfide and oxide forms is that the former requires an oxidant. The oxidant in the present case is biologically generated Fe(III) formed as a metabolite during the activities of the acidophiles. Further, the sulfides of Mo being refractory thereby reduced the leaching kinetics [15]. In addition, Pradhan et al. [11] reported that elemental sulfur forming a layer over Mo matrix could prevent the access of the attacking species.

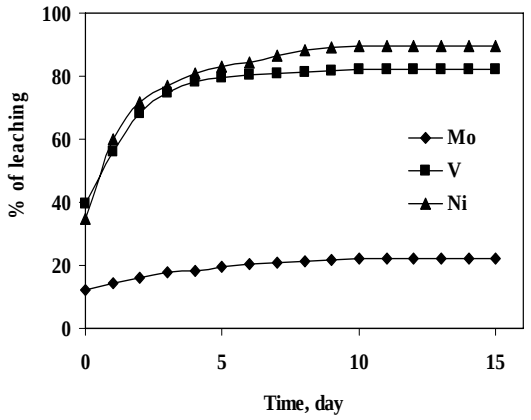

Fig. 1 Effect of contact time on bioleaching efficiency (Conditions: initial Fe(II) conc., 10 g/L; pulp density, 10 % (w/v); initial pH, 2.0; temperature, 35 ^{o}C; particle size, -106 μm; shaking speed,180 rpm)

B. Effect of Fe(II) Concentration

Since Fe(II) is the energy source for the acidophiles, concentration of Fe(II) is an important parameter in determining the bioleaching kinetics. The dissolution process is bacterially assisted, therefore the leaching should depend on the bacterial activity and thus the availability of Fe(II). In addition, Fe(III) being an oxidant, would actively participate during dissolution of sulfide matrix. For that purpose the Fe(II) concentration was varied between 0 to 25 g/L. The results are shown in Fig. 2. It was observed that the leaching rate increased with increase of initial Fe(II) concentration upto 10 g/L and on further increase it showed a negative trend. The decrease of leaching efficiency after a certain Fe(II) concentration may be either due to toxicity of metabolites or formation of a product layer or both. In order to determine the bacterial activity, iron oxidation rates for different initial Fe(II) concentrations were evaluated based on sulfide dissolution under the assumption that dissolution occurred via an indirect mechanism [16] Iron precipitation rate was also calculated simultaneously. The results are shown in Table I. The decrease of iron oxidation rate beyond a certain Fe(II) level may be due to improper adaptation of the bacteria with the leaching media or metabolic toxicity such as an increase in Fe(III) concentration [17]. The iron precipitation rate showed a direct relationship with the initial Fe(II) concentration, i.e. precipitation rate increased with the increase of initial Fe(II) (Table I). The XRD analyses of the leached residues confirmed the precipitated iron to be ammonium jarosite $(NH_4)Fe_3(SO_4)_2(OH)_6$ (data not shown). In all the experiments, pH decreased with time indicating a net production of acid. The generation of acid during leaching was due to iron precipitation as well as oxidation of sulfur. It was further observed that Eh showed an upward trend in all the cases indicating the maintenance of proper oxidizing conditions for the dissolution of the sulfide moiety. Therefore, the decrease of leaching efficiency beyond certain Fe(II) concentration may be due to the formation of product layer as the leaching environment contained sufficient amounts of acid as well as suitable oxidizing conditions for dissolution of oxides and sulfides respectively.

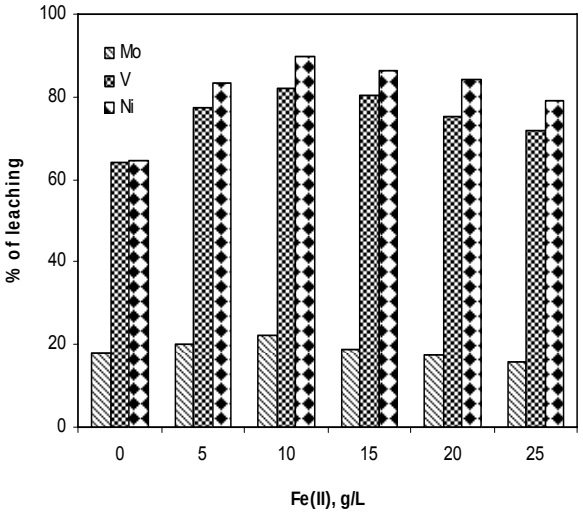

Fig. 2 Efficiency of bioleaching at different initial Fe(II) concentration (Conditions: contact time, 10 days; pulp density, 10 % (w/v); initial pH, 2.0; temperature, 35 ^{o}C; particle size, -106 μm; shaking speed,180 rpm)

TABLE I
IRON OXIDATION AND PRECIPITATION RATE DURING BIOLEACHING FOR DIFFERENT PARAMETERS

Parameters		Iron oxidation rate		Iron precipitation rate	
		Rate, g/L/day	R^2	Rate, g/L/day	R^2
Fe(II) variation, g/L	0	0.075	0.88	-	-
	5	0.114	0.91	0.249	0.93
	10	0.115	0.93	0.711	0.91
	15	0.107	0.91	1	0.99
	20	0.104	0.9	1.36	0.99
	25	0.084	0.88	1.507	0.99
Pulp density, %(w/v)	5	0.124	0.91	0.704	0.89
	10	0.115	0.93	0.711	0.91
	15	0.101	0.96	0.744	0.91
	20	0.094	0.95	0.759	0.91
	25	0.081	0.95	0.784	0.91
pH variation	3	0.081	0.9	0.778	0.99
	2.5	0.096	0.92	0.735	0.97
	2.25	0.109	0.92	0.703	0.96
	2	0.115	0.93	0.711	0.91
	1.75	0.112	0.92	0.211	0.97
	1.5	0.096	0.89	0.009	0.45
Temperature, ^oC	10	0.034	0.99	0.116	0.8
	15	0.051	0.95	0.171	0.94
	20	0.08	0.94	0.194	0.99
	25	0.102	0.95	0.396	0.91
	30	0.114	0.94	0.54	0.92
	35	0.115	0.93	0.711	0.91
Particle size, µm	-212	0.085	0.87	0.69	0.93
	-106	0.115	0.93	0.711	0.91
	-45	0.102	0.86	0.649	0.92

C. Effect of Pulp Density

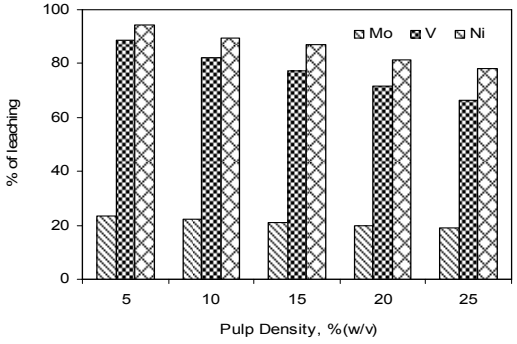

Fig. 3 Effect of pulp density on leaching efficiency of different metals (Conditions: contact time, 10 days; initial Fe(II) conc., 10 g/L; initial pH, 2.0; temperature, 35 ^oC; particle size, -106 µm; shaking speed,180 rpm)

Pulp density is an important parameter involved in determining the process feasibility because a greater pulp density enables use of a smaller reactor. The leaching studies were carried out by varying the pulp density from 5 to 25%. As shown in Fig. 3, the leaching efficiency decreased with the increase of pulp density. This may have occurred due to improper mixing of the particles with the lixiviant, and inadequate diffusion of oxygen which may have decelerated bacterial growth or improper growth of bacteria in higher pulp density. The Eh values of the solution at 5 and 25% pulp density were around 600 and 500 mV respectively, showing less oxidizing condition at higher pulp density. The iron precipitation rate also increased with the increase of pulp density (Table I). Therefore, increase of precipitation rate coupled with decreasing oxidizing condition may have been due to decrease of leaching efficiency with the pulp density.

D. Effect of pH

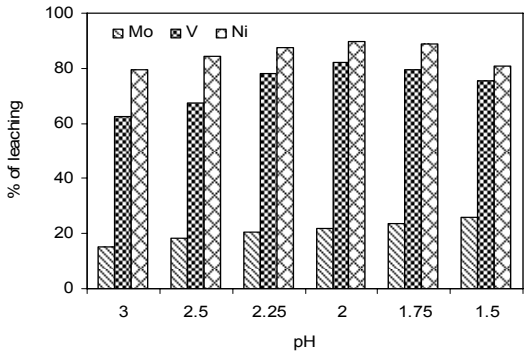

Fig. 4 Effect of initial pH on efficiency (Conditions: initial Fe(II) conc., 10 g/L; pulp density, 10 % (w/v); contact time, 10 days; temperature, 35 ^oC; particle size, -106 µm; shaking speed,180 rpm)

To evaluate the effects of acidity, the initial pH was varied from 1.5 to 3. The leaching efficiency increased with increase of pH up to 2 for Ni and V and thereafter showed a downward trend (as shown in Fig. 4) whereas Mo leaching efficiency decreased with increase of pH. The iron precipitation rate increased with the increase of pH (Table I) and this iron precipitation may be the cause of the decrease of leaching efficiency with the increase of pH. The Eh of the solution in all cases varied in the range 550-650 mV indicating good oxidizing conditions.

E. Effect of Temperature

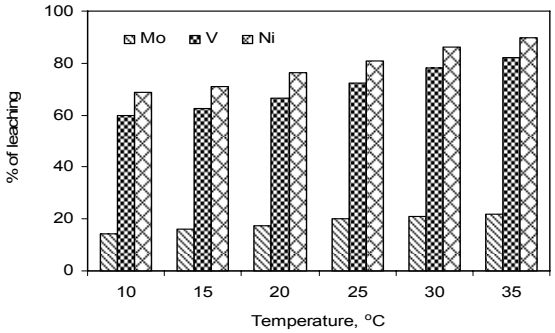

Fig. 5 Effect of temperature on leaching efficiency (Conditions: initial Fe(II) conc., 10 g/L; pulp density, 10 % (w/v); initial pH, 2.0; contact time, 10 days; particle size, -106 µm; shaking speed,180 rpm)

The temperature was varied from 10 to 35^oC. The leaching efficiency increased with the increase of reaction temperature, thus indicating the dissolution process to be endothermic in nature. The leaching results are shown in Fig. 5. The iron oxidation and precipitation rates are shown in Table I. The iron precipitation rate increased with the increase of reaction temperature. The activation energy was calculated from the

Arrhenius equation by plotting ln(reaction rate) versus 1/Temperature [18]. From the slope, the of activation energies for different metals were calculated. The activation energies for Ni, V and Mo were calculated to be 3.1, 5.2 and 11.4 kJ/mole, respectively. Based on these activation energies it can be concluded that the dissolution process followed a mixed kinetic reaction [18].

F. Effect of Particle Size

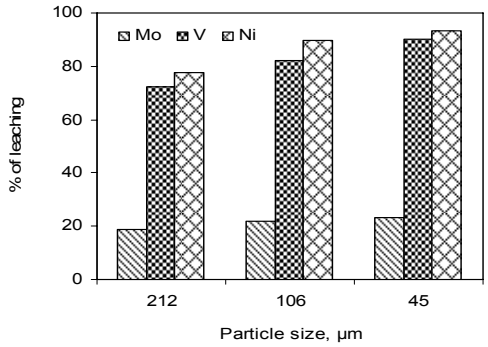

Fig. 6 Effect of particle size on leaching efficiency (Conditions: initial Fe(II) conc., 10 g/L; pulp density, 10 % (w/v); initial pH, 2.0; contact time, 10 days; temperature, 35 ^{o}C; shaking speed,180 rpm)

Bacterial leaching studies were carried out for three different particle sizes, namely-45, -106 and -212 µm. The leaching efficiency increased with the decrease of particle size as shown in Fig. 6. The iron oxidation and precipitation rates are shown in Table I. The increase of leaching efficiency with the decrease of particle size is due to the increased surface area when smaller particles were used.

G. Evaluation of Kinetic Model

The dissolution rates were found to depend on various leaching parameters. The XRD analyses of the leached residue showed the presence of ammonium jarosite $(NH_4)Fe_3(SO_4)_2(OH)_6$ as a product layer. If the leaching process is controlled by diffusion and the product layer, as well as the elemental sulfur, are impervious to attacking species, then the leaching kinetics can be written as follows [18]:

$$k_p t = 1 - \frac{2}{3}x - (1-x)^{\frac{2}{3}} \quad (1)$$

where, k_p = parabolic rate constant
t = time
x = fraction reacted

Alternatively, if the product layer as well as sulfur is porous, then it would not hinder the attacking species and the dissolution process would be controlled by the shrinking core particle model [18]. Therefore, the kinetic equation can be written as follows:

$$k_c t = 1 - (1-x)^{\frac{1}{3}} \quad (2)$$

where, k_c = rate constant
t = time
x = fraction reacted

The diffusion model requires a plot of $1-2/3x-(1-x)^{2/3}$ versus t would give a straight line where the slope would be k_p. Similarly, for a shrinking core model, a plot of $1-(1-x)^{1/3}$ versus t would give a straight line and the slope would be k_c. Both the model equations are used to determine the nature of the product layer and the results are shown in Figs. 7 and 8. From the figures, it can be observed that the slopes of the diffusion control models are passing through zero unlike the shrinking core particle model. Furthermore, the R^2 values indicated that the product layer is impervious and therefore rate determining (Table II).

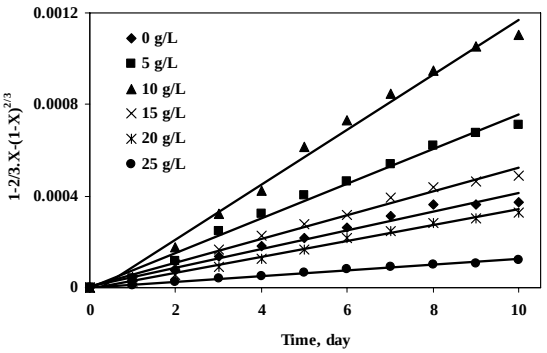

Fig. 7 Diffusion control for different initial Fe(II) concentration

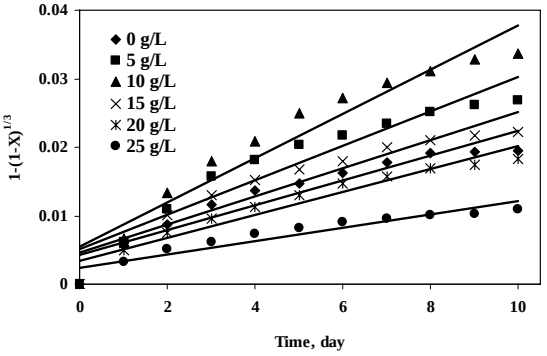

Fig. 8 Chemical control for different initial Fe(II) concentration

IV. Conclusion

In this study, experiments were conducted to evaluate the leaching efficiency of Ni, V and Mo from spent petroleum catalyst using iron oxidizing bacteria. The dissolution process followed dual kinetics, i.e. an initial faster rate followed by a slower one, attaining equilibrium after 10 days of reaction time. The initial concentration of Fe(II) played an important role in determining the leaching efficiency. The leaching efficiency showed an upward trend up to 10 g/L Fe(II) concentration and then downward on further increase of Fe(II) concentration. This may be due to the increase of iron precipitation rate. The leaching efficiency decreased with increase of pulp density, probably due to improper mixing or an increase of iron precipitation rate or a lack of oxygen or combination of all these factors. Acidity and particle size also played an important role in determining the leaching efficiency. The activation energy favored a mixed kinetics model. The

dissolution reaction followed a product layer diffusion controlled mechanism. The diffusivity coefficients for Ni, V and Mo dissolutions were also calculated.

TABLE II
RATE CONSTANTS OF DIFFUSION CONTROL AND SHRINKING CORE MODEL FOR NI, V AND MO

	Nickel				Vanadium				Molybdenum			
	Diffusion control		Chemical control		Diffusion control		Chemical control		Diffusion control		Chemical control	
	k_p x10^3	R^2	k_c x10^2	R^2	k_p x10^3	R^2	k_c x10^2	R^2	k_p x10^5	R^2	k_c x10^3	R^2
Fe(II) variation, g/L												
0	1.2	.9	0.97	.8	0.9	.96	0.86	.89	0.4	.98	1.8	.9
5	3.4	.9	1.68	.8	2	.86	1.27	.76	8	.99	2.5	.91
10	4.4	.9	1.89	.8	2.5	.81	1.39	.7	10	.99	3.2	.93
15	4	.9	1.82	.8	2.3	.84	1.35	.73	5	.99	2	.9
20	3.5	.9	1.7	.8	1.7	.82	1.14	.71	3	.99	1.7	.93
25	2.9	.9	1.56	.8	1.5	.89	1.08	.78	1	.99	1	.89
Pulp density, %(w/v)												
5	5.1	.9	2.06	.8	3.4	.85	1.67	.74	20	.98	3.6	.91
10	4.4	.9	1.89	.8	2.5	.81	1.39	.7	10	.99	3.2	.92
15	4.3	.9	1.85	.8	1.9	.77	1.19	.66	10	.99	3	.92
20	3.7	.9	1.71	.8	1.5	.79	1.05	.67	8	.99	2.6	.94
25	3.6	.9	1.69	.8	1.3	.79	0.99	.68	6	.99	2.4	.96
pH variation												
3	2.8	.9	1.51	.8	0.7	.97	0.72	.86	1	.87	0.8	.69
2.5	3.5	.9	1.69	.8	1	.86	0.82	.72	4	.95	1.7	.82
2.25	4.1	.9	1.82	.8	2.1	.9	1.27	.77	8	.99	2.7	.92
2	4.4	.9	1.89	.8	2.5	.81	1.39	.7	10	.99	3.2	.92
1.75	4.2	.9	1.85	.8	2.2	.81	1.29	.7	20	.99	3.7	.89
1.5	2.8	.9	1.46	.7	1.7	.88	1.12	.74	20	.98	4.3	.87
Temperature, ^oC												
10	1.5	.9	1.08	.8	0.5	.88	0.6	.75	0.4	.93	0.6	.97
15	1.7	.9	1.13	.8	0.6	.89	0.68	.74	2	.98	1.3	.97
20	2.3	.9	1.34	.8	0.9	.86	0.79	.71	3	.99	1.7	.96
25	2.9	.9	1.51	.8	1.4	.92	1.01	.77	7	.99	2.6	.96
30	3.9	.9	1.76	.8	2	.83	1.24	.71	10	.98	3	.97
35	4.4	.9	1.89	.8	2.5	.81	1.39	.7	10	.99	3.2	.95
Particle size, μm												
212	2.8	.9	1.44	.7	1.6	.93	1.07	.78	0.6	.98	2.4	.94
106	4.4	.9	1.89	.8	2.5	.81	1.39	.7	10	.99	3.2	.93
45	4.7	.8	1.92	.7	3.3	.88	1.64	.75	10	.99	3.4	.91

ACKNOWLEDGMENT

This work was supported by the Korea Foundation for International Cooperation of Science & Technology (KICOS) through a grant provided by the Korean Ministry of Science & Technology (MOST) in 2009 (No. K20602000004-08E0200-00410).

REFERENCES

[1] Marafi M., Stanislaus A. Spent catalyst waste management: A review Part-I-Developments in hydroprocessing catalyst waste reduction and use. Res. Cons. Rec. 52:859-873(2008).
[2] United States Environmental Protection Agency (USEPA). Hazardous waste management system. Federal Register 68(202), 55935-5994(2003).
[3] Medvedev A.S., Malochkina N.V. Sublimation of molybdenum trioxide from exhausted catalyst employed for the purification of oil products. Rus. J. Non-ferrous Met. 48:114-117(2007).
[4] Gaballah I., Diona M. Valuable metals recovery from spent catalyst by selective chlorination. Res. Cons. Rec. 10:87-96(1994).
[5] Parkinson G., Isho S. Recyclers try new ways to process spent catalyst. Chem. Eng. 94:25-31(1987).
[6] Park K.H., Mohapatra D., Nam C.W. Two stage leaching of activated spent HDS catalyst and solvent extraction of Al using organo-phosphinic extractant, Cyanex-272. J. Haz. Mat. 148:287-295(2007).
[7] Kar B.B., Datta P., Misra V.N. Spent catalyst: Secondary source for Mo recovery. Hydromet. 72:87-92(2004).
[8] Lee F.M., Knudse R.D., Kidd D.R. Reforming catalyst made from the metals recovered from spent atmospheric residue desulphurization catalyst. Ind. Eng. Chem. Res. 31:487-490(1992).
[9] Siemens R.E., Jong B.W., Russel J.H. Potential of spent catalyst as a source of critical metals. Cons. Rec. 9:189-196(1986).
[10] Pradhan D., Mishra D., Kim D.J., Roychaudhury G., Lee S.W. Dissolution kinetics of spent petroleum catalyst using two different acidophiles. Hydromet. 99:157-162(2009).
[11] Pradhan D., Mishra D., Kim D.J., Ahn J.G., Roychaudhury G., Lee S.W. Bioleaching kinetics and multivariate analysis of spent petroleum catalyst dissolution using two acidophiles. J. Haz. Mat. (in press).
[12] Aung K.M.M., Ting Y.P. Bioleaching of spent fluid catalytic cracking catalyst using Aspergillus niger. Journal of Biotechnology 116: 59-170(2005).
[13] Bosio V., Viera M., Donati E. Integrated bacterial process for the treatment of a spent nickel catalyst. Journal of Hazardous Materials 154:804–810(2008).
[14] Silverman M.P., Lundgren D.G. Studies on the chemoautotrophic iron bacterium Ferrobacillus ferrooxidans. I. An improved medium and harvesting procedure for securing high cell yields. J. Bacteriol. 77:642-647(1959).
[15] Olson G.J., Clark T.R. Bioleaching of molybdenite. Hydromet. 93:10-15(2008).
[16] Boon M., Snijder M., Hansford G.S., Heijnen J.J. The oxidation kinetics of ZnS with Thiobacillus ferrooxidans. Hydromet. 48:171-186(1998).
[17] Das T., Ayyappan S., RoyChaudhury G.. Factors affecting bioleaching kinetics of sulfide ores using acidophilic microorganisms. Biomet. 12:1-10(1999).
[18] Sohn H.Y., Wadsworth M.E. Rate process of extractive metallurgy, Plenum Press, New York, 1979.